

# Flow Development and Analysis of MHD Generators and Seawater Thrusters

E. D. Doss

Argonne National Laboratory,  
Argonne, Illinois 60439  
Mem. ASME

G. D. Roy

Office of Naval Research,  
Arlington, VA 22217  
Mem. ASME

The flow characteristics inside magnetohydrodynamic (MHD) plasma generators and seawater thrusters are analyzed and are compared using a three-dimensional computer model that solves the governing partial differential equations for fluid flow and electrical fields. Calculations have been performed for a Faraday plasma generator and for a continuous electrode seawater thruster. The results of the calculations show that the effects caused by the interaction of the MHD forces with the fluid flow are strongly manifested in the case of the MHD generator as compared to the flow development in the MHD thruster. The existence of velocity overshoots over the sidewalls confirm previously published results for MHD generators with strong MHD interaction. For MHD thrusters, the velocity profile is found to be slightly flatter over the sidewall as compared to that over the electrode wall. As a result, distinct enhancement of the skin friction exists over the sidewalls of MHD generators in comparison to that of MHD thrusters. Plots of velocity profiles and skin friction distributions are presented to illustrate and compare the flow development in MHD generators and thrusters.

## 1 Introduction

Extensive work has been done on channel flow inside open-cycle MHD plasma generators (e.g., Roy and Wu, 1975; Doss and Curry, 1976; Doss et al., 1975, 1981; Ahluwalia and Doss, 1980; Doss and Ahluwalia, 1983; Vanka and Ahluwalia, 1982, 1983), but there has been minimal research effort on duct flow inside MHD seawater thrusters (e.g., Phillips, 1962; Doragh, 1963; Way, 1968; Saji, et al., 1978; Hummert, 1979; Cott et al., 1988). However, MHD flow inside those ducts is subject to  $J \times B$  forces whether the duct is an MHD generator or an accelerator. For MHD generators, electrical power is extracted from the interaction of the fluid flow with the magnetic field. For MHD thrusters, energy is supplied to the duct by applying an external electrical field, and the resulting electrical currents interact with the magnetic field to produce a driving force that pushes the fluid through the duct. There are obviously some differences between the flow medium and the operating conditions between the two applications; however, the governing equations and the physical phenomena are quite similar. Figure 1 is a schematic diagram of the concept of MHD plasma generator and seawater thruster.

The literature on MHD channel flow for plasma open-cycle generators indicate that the flow and electrical fields in MHD generators are inherently three-dimensional for a variety of reasons. The interaction of the MHD electrical forces ( $J \times B$ ) with the fluid flow leads to flow distortions (Vanka and Ahluwalia, 1982, 1983; Doss and Ahluwalia, 1983). The cross-sectional nonuniformity of the axial component of the Lorentz

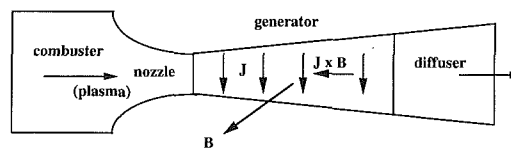


Fig. 1(a) A schematic diagram of an MHD generator

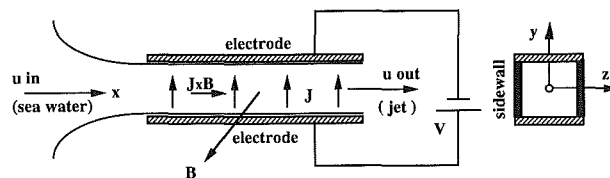


Fig. 1(b) A schematic diagram of an MHD generator

force ( $J, B$ ) is directly responsible for the generation of velocity overshoots in the boundary layers. The nonuniformity in the magnetic field direction of the Lorentz force due to Hall current ( $J_x B$ ) produces secondary flows which in turn leads to flow asymmetry.

For MHD seawater thrusters, however, the electrical conductivity of seawater is expected to be practically uniform across and along the thruster provided the effect of bubbles formation, due to electrolysis, on the electrical conductivity is minimum. The Hall parameter for seawater thruster is also negligible. Therefore, one might anticipate that such flow non-uniformities would not be manifested strongly inside the ducts as much as in the case of plasma generators. In order to in-

Contributed by the Fluids Engineering Division for publication in the JOURNAL OF FLUIDS ENGINEERING. Manuscript received by the Fluids Engineering Division September 25, 1990.

investigate the extent of such flow nonuniformities in the MHD thrusters, three-dimensional calculations of the flow and electrical fields have to be carried out.

The purpose of the present paper is to report the results of a comparative analysis performed using the three-dimensional flow model that has been previously developed, and to present a comparison of the development of the flow fields inside MHD generators and seawater thrusters.

## 2 MHD Three-Dimensional Generator and Thruster Model

A three-dimensional MHD generator model incorporating fully the interaction between the flow and the electrical fields inside the channel has been developed at Argonne National Laboratory and has been applied for several open-cycle MHD generators (Vanka and Ahluwalia, 1982, 1983; Doss and Ahluwalia, 1983).

Therefore, only a brief description of this model is given in this paper for completeness. The details of the model, flow equations, and their methods of solution are discussed in the references. (Vanka and Ahluwalia, 1982, 1983; Vanka et al., 1982). The flow fields are represented by the parabolic form of the three-dimensional compressible, turbulent Navier-Stokes equations and their solution is coupled to the solution of the electrical field in the cross-flow direction. The equations solved in this model consist of the mass conservation equation, the three momentum equations, the equations for enthalpy, turbulence kinetic energy and dissipation rate, the Maxwell and Ohms law equations. This set of coupled equations is solved by the use of a finite-difference calculation procedure. The turbulence is represented by a two-equation model of turbulence in which partial differential equations are solved for the turbulence kinetic energy and its dissipation rate.

The three-dimensional model has been adapted for the application of seawater thrusters. A continuous electrode configuration has been used in this application where the electric field along the flow direction is assumed to be zero. This assumption is reasonable since the Hall parameter for seawater is negligible. An applied electric field, in terms of a load factor, is specified as the boundary condition for the electrode walls. This assumption is also reasonable for seawater thruster of constant cross section, because the average axial velocity is constant at any cross section for mass conservation. The sidewalls are assumed to be insulators. The electrical fields are computed at each cross sectional plane perpendicular to the flow. Locally, the axial variation of the electrical fields and current densities are assumed to be negligible in comparison with their variations in the cross plane. This assumption may not be accurate where there are strong variations of the magnetic field and/or the flow velocity, or where there are abrupt changes in the boundary conditions. Such situations may exist

near the ends of the MHD thrusters; however, they are beyond the scope of this paper.

## 3 Applications and Results

**3.1 Operating Conditions.** Computations have been performed using the three-dimensional model described in the previous section for an MHD plasma generator operating in the Faraday mode with insulating sidewalls, and for an MHD thruster operating in the continuous electrode mode with insulating sidewalls. The general operating parameters for the applications considered are listed in Table 1. The flow at the entrance of the generator and thruster is assumed to be a plug flow.

The physical properties of seawater are documented by Parker (1987) and the values used are for a temperature of 20°C, while those for plasma are obtained from the NASA-Lewis Chemical equilibrium code.

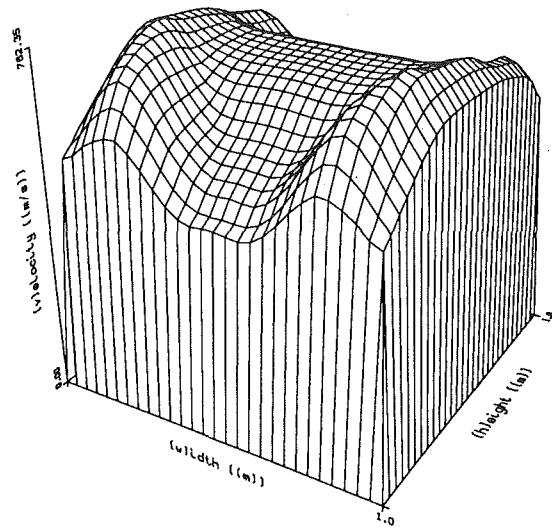
**3.2 Grid Resolution and Sensitivity of the Predictions.** For MHD generators, the theoretical predictions of the three-dimensional MHD model have been compared previously by Vanka and Ahluwalia (1983), for a generator operating in the Faraday mode. Excellent agreement was reported between the theory and experiments. For that particular application the calculations were made with a  $29 \times 29$  finite-difference grid in the cross section and with a forward step of 2 cm.

In the current applications for MHD thrusters, the sensitivity of the predictions to the grid-size and to the forward step-size has been investigated. For example, for the same operating conditions of the thruster (magnetic field  $B = 20$  T, load factor  $K = 1.5$ , flow velocity  $u = 30$  m/s), several computer runs have been performed with  $15 \times 15$ ,  $29 \times 29$ , and  $39 \times 39$  finite-difference grids in the cross section and with a forward step of 4 cm. The grid-size distribution across the thruster has been defined using a power-law function with an exponent  $py = 2$ . [the distance away from the wall,  $y(i) = (\text{height}/2) * (i/i_{cl})^{2p}$ , where  $i = 0$  is at the wall and  $i_{cl}$  is the index of the grid at the centerline]. The initial step size away from the wall for the three above mentioned finite-difference grids is .0102, 0.00255, and 0.00139 m, respectively. Three variables have been used to investigate the sensitivity of the results using the different grids and those variables are the pressure rise along the 10 m thruster, the total frictional losses, and the total input power. It has been found that the predicted total input power and the pressure rise along the thruster remain practically the same, i.e., insensitive to the number of grids. For the total frictional losses, there is only 0.8 percent difference between the predictions using the  $29 \times 29$  and the  $39 \times 39$  grids and 5.3 percent between the predictions using the  $15 \times 15$  and  $39 \times 39$  grids.

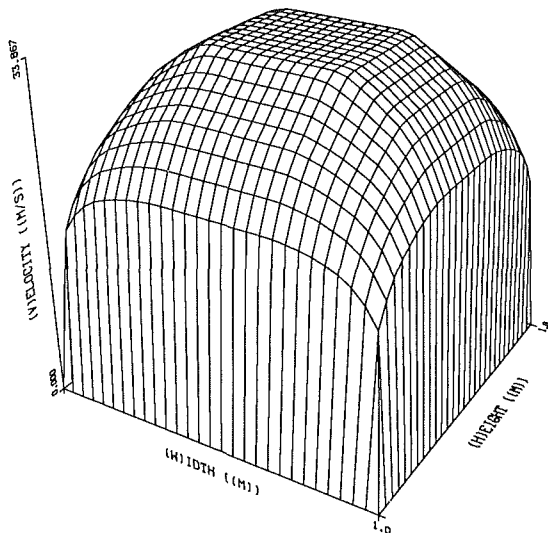
Several other computations have been performed using  $29 \times 29$  and  $39 \times 39$  finite-difference grids and with forward

**Table 1 Operating condition for the illustrated examples**

	Generator	Thruster	
Geometry	rectangular	rectangular	
• length	10	10	m
• height $\times$ width (inlet)	$0.5 \times 0.5$	$1.0 \times 1.0$	$m^2$
• height $\times$ width (outlet)	$1.0 \times 1.0$	$1.0 \times 1.0$	$m^2$
• wall roughness	2.5	2.5	mm
Wall temperature	1800	300	K
Inlet fluid temperature	2760	300	K
Working fluid	Products of combustion of natural gas seeded with potassium	Seawater	
• electrical conductivity	7.2-5.1	4.8	S/m
Inlet flow velocity	770	30	m/s
Mass flow rate	75	30750	Kg/s
Magnetic field	6	20	T
Duct loading	Faraday with insulating sidewalls	continuous electrode with insulating sidewalls	
• average electric load factor	0.2-0.95	1-20	



A. Generator



B. Thruster

Fig. 2 Surface plots of the axial velocity distribution at the exit of the MHD generator and thruster ( $x = 10$  m)

step sizes of 10, 4, and 2 cm. For this particular application, where the magnetic field and the average flow velocity are constants along the thrusters, the predictions of the pressure rise, total frictional losses and input power are found to be practically the same (less than 0.8 percent difference) for the three quoted step sizes.

Based on these findings and using previous experience in analyzing the performance of MHD generators (Vanka and Ahluwalia, 1982, 1983; Vanka, et al., 1982), the following parametric study has been performed using a  $29 \times 29$  finite-difference grid in the cross section and with a 4 cm forward step.

**3.3 Flow Fields and Friction Factor.** A Parametric study has been performed by varying the average electric load factor ( $K \equiv \langle E_y \rangle / \langle uB \rangle$  where  $E_y$  is the Faraday electric field) between 0.0 and 0.95 ( $K < 1.0$ ) for the MHD generator and between 1 and 20 ( $K > 1.0$ ) for the thruster. Sample results are presented and discussed in this paper for an MHD generator operating with  $K = 0.75$  and for an MHD thruster operating with  $K = 2$ . More details can be found in Vanka and Ahluwalia (1983) and Doss and Roy (1991).

Figure 2 shows surface plots for the calculated axial velocity

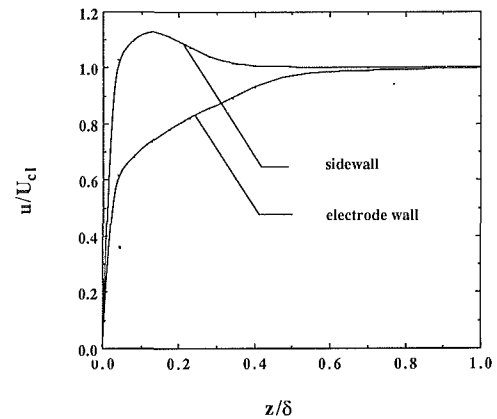


Fig. 3 Normalized velocity profiles across the MHD generator walls ( $x = 8$  m)

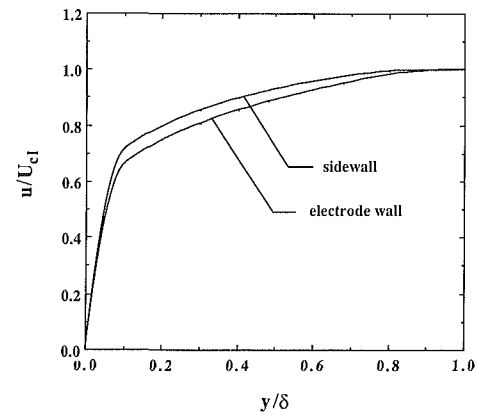


Fig. 4 Normalized velocity profiles across the MHD thruster walls ( $x = 8$  m)

distributions at the exit cross-sections ( $x = 10$  m) of the MHD generator and thruster. As shown on Fig. 2, the three-dimensional effects, caused by the interaction of the Lorentz forces ( $\mathbf{J} \times \mathbf{B}$ ) with the fluid flow, are strongly manifested in the case of the MHD generator as compared to the flow development in the thruster. The axial component of the Lorentz force ( $J_y B$ ) acts as a retarding force for the case of the generator, while it acts as an accelerating force for the case of the thruster. The  $J_y B$  force, however, is not uniform over the cross-section. As a result, velocity distortions exist and they are manifested strongly as velocity overshoots in the boundary layer for the MHD generator case. Furthermore, the perpendicular component of the Lorentz force ( $J_x B$ ) produces cross stream transverse velocities leading to flow asymmetries. For MHD seawater thrusters, operating in the continuous electrode mode and with a negligible Hall parameter, the  $J_x B$  component is practically non-existent. Therefore, as shown in Fig. 2, the flow structure for the thruster is less complex than that for the generator.

Figures 3 and 4 present the corresponding axial velocity profiles in the boundary layer for the two devices. At first, one may think that the surface plot for the thruster (Fig. 2) is typical to normal non-MHD turbulent flow. However, as shown on Fig. 4, there is a difference between the shape of the axial velocity profile along the electrode wall and that along the sidewall. The velocity near the insulating wall (Hartmann boundary layers) is relatively higher than that near the electrode walls. For the generator, the disparity between the velocity profiles over the two walls is much larger where there is a distinct velocity overshoot in the boundary layers.

Figure 5 presents the corresponding variation of the  $J_y$ -com-

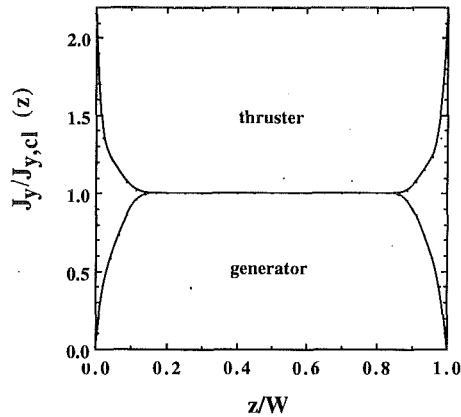


Fig. 5 Normalized current density across the sidewalls of the MHD generator and thruster ( $x = 8$  m)

ponent of the current density across the duct between the insulating walls for the MHD generator and thruster. The nonuniform  $J_y$ -distribution acts on the flow differently. For the case of the generator, where the electrical conductivity is very small in the boundary layers in comparison to the main flow,  $J_y$  is correspondingly very small compared to the core flow values. Accordingly, the retarding  $J_y B$  force exerts a less force on the sidewall (Hartmann) boundary layer. In a relative sense, the sidewall boundary layers are accelerated in relation to the central region. This relative acceleration of the sidewall boundary layers results in the observed velocity overshoots.

On the other hand, for the MHD thruster case, the seawater electrical conductivity is practically constant (neglecting the effects of bubble formation). Therefore, any change of the current density,  $J_y$ , in the sidewall (Hartmann) boundary layers will be caused by the nonuniformity of the velocity. For constant electrical potential between the cathode and the anode, the current density is larger in the sidewall boundary layers because of the smaller velocities. Therefore, a larger accelerating force ( $J_y B$ ) will be felt on the flow in the sidewall boundary layers as compared to the main flow due to the increase of the current density component  $J_y$  as shown in Fig. 5. Consequently, the velocity profile is flatter over the sidewall in comparison to the velocity profile in the boundary layers over the electrode wall (Fig. 4).

As a result of such nonuniformities in the flow fields, non-uniform distribution of the skin friction is expected along the duct walls. Figures 6 and 7 present the variation of the friction factor ( $C_f$ ) along the electrode wall and the sidewall of the MHD generator and thruster, respectively. The skin friction is higher on the sidewall for both applications but with a distinct difference for the generator case. Wall friction can have a strong adverse effect on the performance of both MHD devices (generator and thruster) in terms of their electrical efficiency. Such an important issue has been discussed recently in detail for MHD thrusters by Doss and Geyer (1990). Therefore greater attention should be given to the calculation of the flow fields and the frictional losses for those applications.

### Summary and Conclusions

1. A three-dimensional MHD computer model has been applied to compare the flow characteristics inside MHD plasma generators with those inside seawater thrusters. Computations have been performed for a Faraday plasma generator operating with a 6 Tesla magnet and at a load factor  $K = 0.75$ , and for an MHD thruster operating in the Faraday mode with continuous electrodes with a 20 Tesla magnet and at a load factor  $K = 2.0$ .

2. The three-dimensional effects caused by the interaction

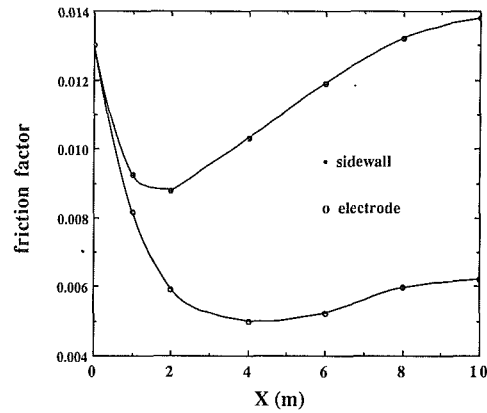


Fig. 6 Variation of the friction factor along the duct walls of the MHD generator

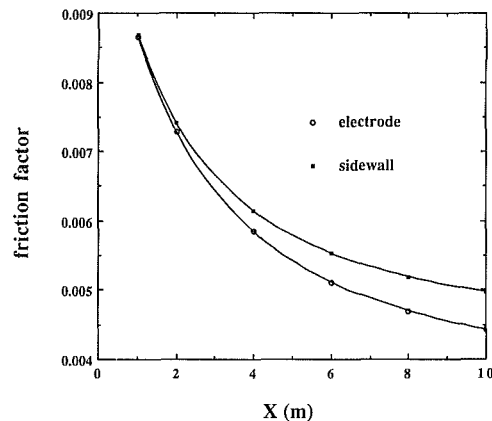


Fig. 7 Variation of the friction factor along the duct walls of the MHD thruster

of the Lorentz forces ( $J \times B$ ) with the fluid flow are strongly manifested in the MHD generator as compared to the flow development in the thruster. Distinct velocity overshoots exist in the sidewall boundary layers for the case of the generators, whereas for the thruster a slightly flatter boundary layer velocity profile exists over the sidewall boundary layer as compared to the velocity profile over the electrode wall.

3. The flow velocity nonuniformities in both applications is caused basically by the nonuniformities of the component of the current density  $J_y$  in the Hartmann layers of the sidewalls of the MHD ducts. For MHD plasma generators the nonuniform  $J_y$ -distribution in the Hartmann layers is primarily caused by the strong variation of the electrical conductivity and secondarily by the nonuniformity of the velocity in the boundary layers. For MHD seawater thrusters, the electrical conductivity is uniform. Therefore, the nonuniformities of  $J_y$  in the sidewall boundary layers are caused primarily by the nonuniformities of the velocity in those layers.

4. As a result of such velocity nonuniformities, nonuniform distributions of the skin friction exist along the duct walls. The friction coefficient is higher on the sidewalls for both applications but with a distinct difference for the generator case.

### Acknowledgment

This work has been sponsored by the Office of Naval Research, U.S., under Contract No. N00014-89-F-0064.

### References

Ahluwalia, R. K., and Doss, E. D., 1980, "Quasi-Three Dimensional Modeling of Flow in MHD Channels," *Numerical Heat Transfer*, Vol. 3, pp. 67-87.

- Cott, D. W., Daniel, V. W., Carrington, R. A., and Herring, J. S., 1988, "MHD Propulsion For Submarines," *CDIF External Report*, No. 2, DOE-MHD-D140, MSE Inc., Butte, Montana.
- Doragh, R. A., 1963, "Magnetohydrodynamic Ship Propulsion Using Superconducting Magnets," *Proceedings of Naval Architects and Marine Engineers Transaction*, Vol. 71.
- Doss, E. D., Argyropoulos, G. S., and Demetriades, S. T., 1975, "Two-Dimensional Flow Inside MHD Ducts with Transverse Asymmetries," *AIAA Journal*, Vol. 13, No. 5, pp. 545-546.
- Doss, E. D., and Curry, B. P., 1976, "Studies of the 3-D Coupled Flows Between the Electrode and Sidewalls of MHD Channels," *AIAA Paper*, No. 76-311, AIAA 9th Fluid and Plasma Dynamics Conference.
- Doss, E., Geyer, H., Ahluwalia, R. K., and Im, K., 1981, "Two-Dimensional Performance Analysis and Design of MHD Channels," *ASME JOURNAL OF FLUIDS ENGINEERING*, Vol. 103, pp. 307-314.
- Doss, E. D., and Ahluwalia, R. K., 1983, "Three-Dimensional Flow Development In MHD Generators At Part Load," *Journal of Energy*, Vol. 7, No. 4, pp. 289-290.
- Doss, E. D., and Geyer, H. K., 1990, "Effects of Friction and End Losses on MHD Thruster Efficiency," *Proceedings of the 28th Engineering Aspects of Magnetohydrodynamics*, Chicago, Ill., pp. III.2.1-III.2.8.
- Doss, E. D., and Roy, G. D., 1991, "Flow Characteristics Inside MHD Seawater Thrusters," *Journal of Propulsion and Power*, Vol. 7, No. 4, pp. 635-641.
- Hummert, G. T., 1979, "An Evaluation of Direct Current Electromagnetic Propulsion In Seawater," *Report ONR-CR168-007-1*, Westinghouse Research Laboratories, Pittsburgh, Pennsylvania.
- Parker, S. P., ed., 1987, *McGraw-Hill Encyclopedia of Science and Technology*, McGraw-Hill, New York, 6th Edition, Vol. 16, pp. 144-178.
- Phillips, O. M., 1962, "The Prospects for Magnetohydrodynamic Ship Propulsion," *Journal of Ship Research*, Vol. 43, pp. 43-51.
- Roy, G. D., and Wu, Y. C. L., 1975, "Study of Pressure Distribution Along Supersonic Magnetohydrodynamic Generator Channel," *AIAA Journal*, Vol. 13, No. 9, pp. 1149-1153.
- Saji, Y., Kitano, M., and Iwata, A., 1978, "Basic Study of Superconducting Electromagnetic Thrust Device for Propulsion in Sea Water," *Advances in Cryogenic Engineering*, Timmerhans, K. D., ed., Vol. 23, pp. 159-169.
- Vanka, S. P., Ahluwalia, R. K., and Doss, E. D., 1982, "Three-Dimensional Analysis of MHD Generators and Diffusers," *Argonne National Laboratory*, Report No. ANL/MHD-82-4, Argonne, Ill.
- Vanka, S. P., and Ahluwalia, R. K., 1982, "Three-Dimensional Flow and Thermal Development in Magnetohydrodynamic Channels," *Journal of Energy*, Vol. 6, No. 3, pp. 218-224.
- Vanka, S. P., and Ahluwalia, R. K., 1983, "Coupled Three-Dimensional Flow and Electrical Calculations for Faraday MHD Generators," *Journal of Energy*, Vol. 7, No. 1, pp. 65-72.
- Way, S., 1968, "Electromagnetic Propulsion for Cargo Submarines," *Journal of Hydraulics*, Vol. 2, No. 2, pp. 49-57.